Special Issue "Recent Progress in Seismo Electromagnetics" in Physics and Chemistry of the Earth

A. Takeuchi, B.W.S. Lau, F.T. Freund

Current and surface potential induced by stress-activated positive holes in igneous rocks

Akihiro Takeuchi[1,2] *, Bobby W. S. Lau[2], and Friedemann T. Freund[2,3]

[1]*Department of Chemistry, Faculty of Science, Niigata University, 8050 Ikarashi-ninocho, Niigata 950-2181, Japan*
[2]*Department of Physics, San Jose State University, One Washington Square, San Jose, CA 95192-0106, USA*
[3]*GEST Fellow, Planetary Geodynamics Laboratory, NASA Goddard Space Flight Center, Greenbelt MD 20771, USA*

* Corresponding author:
Department of Chemistry, Faculty of Science, Niigata University
8050 Ikarashi-ninocho, Niigata 950-2181, Japan
tel: 81-25-262-6169
fax: 81-25-262-6116
e-mail: takeuchi@curie.sc.niigata-u.ac.jp

Abstract

In order to model seismo-electromagnetic phenomena, we focus on one specific defect as an alternative source of charge carriers in igneous rocks. These charge carriers are defect electrons in the O^{2-} sublattice that are chemically equivalent to O^- in a matrix of O^{2-} and are known as positive holes (p-holes). They are activated from peroxy defects: $O_3X–OO–XO_3$ (X = Si, Al etc.) that are known as positive hole pairs (PHPs). Stressed igneous rocks behave like p-type semiconductors. In order to examine the contributions of p-holes to seismo-electromagnetic phenomena, we conducted two series of uniaxial loading tests using air-dry tiles of several types of rocks (granite, anorthosite, gabbro, limestone, and marble) and glass. We observed that the igneous rock tiles under centrally loading generated (1) a positive current, carried by holes and flowing from the central stressed volume through the surrounding unstressed volume to the edges of the tiles and (2) a negative current, carried by electrons and flowing from the central stressed volume into the load pistons. In addition, a positive potential appeared on the surface of the unstressed portion of the igneous rock tiles. On the other hand, limestone containing small amounts of silicate grains generated lower currents. Marble containing no silicate grains and glass generated much lower and no currents, respectively. The current generated per 1 m^3 of stressed volume at a rapid loading up to 50 MPa was on the order of 10^{-5} A for granite. A slow increase of the stress level by 10 MPa superimposed on the 50 MPa added a 10^{-6} A of the current. Anorthosite and gabbro showed 10–50 times higher currents, and limestone and marble showed 1/10–1/100 times. The vertical electric field during a stress change from 50 MPa to 60 MPa was on the order of 10^2 V/m. We propose that, when stresses and strain change at or around a fault zone before and during an earthquake, similar currents and electric fields will be generated in and on the ground, respectively. Such currents and fields will be accompanied by changes in the conductivity of the rocks and may lead to abnormal electromagnetic fields and emissions and to ionospheric perturbations.

Keywords: Seismo-electromagnetic phenomena; uniaxial loading; igneous rock; positive hole (p-hole); p-type semiconductor.

1. Introduction

Seismo-electromagnetic phenomena such as Earth currents and conductivity changes, abnormal electromagnetic fields and emissions, and ionospheric perturbations have been of interest to Earth and Planetary scientists and engineers (e.g., Gokhberg et al., 1995; Hayakawa, 1999; Hayakawa and Molchanov, 2002; Pulinets and Boyarchuk, 2004; Varotsos, 2005 and references therein). The effects point to telluric currents. To explain such currents, a variety of possible sources have been proposed: piezoelectric potentials of quartz (e.g., Ogawa and Utada, 2000; Yoshida and Ogawa, 2004), streaming potentials by moving ground water (e.g., Mizutani et al., 1976; Kormiltsev et al., 1998), emanation of special gases (e.g., Sorokin et al., 2001; Rapoport et al., 2004), tribological electromagnetics (e.g., Enomoto and Hashimoto, 1990; Takeuchi et al., 2004), and moving dislocations (e.g., Hadjicontis and Mavromatou, 1994, 1995; Teisseyre, 2001; Varotsos et al., 2001). In contrast, we have identified an alternative

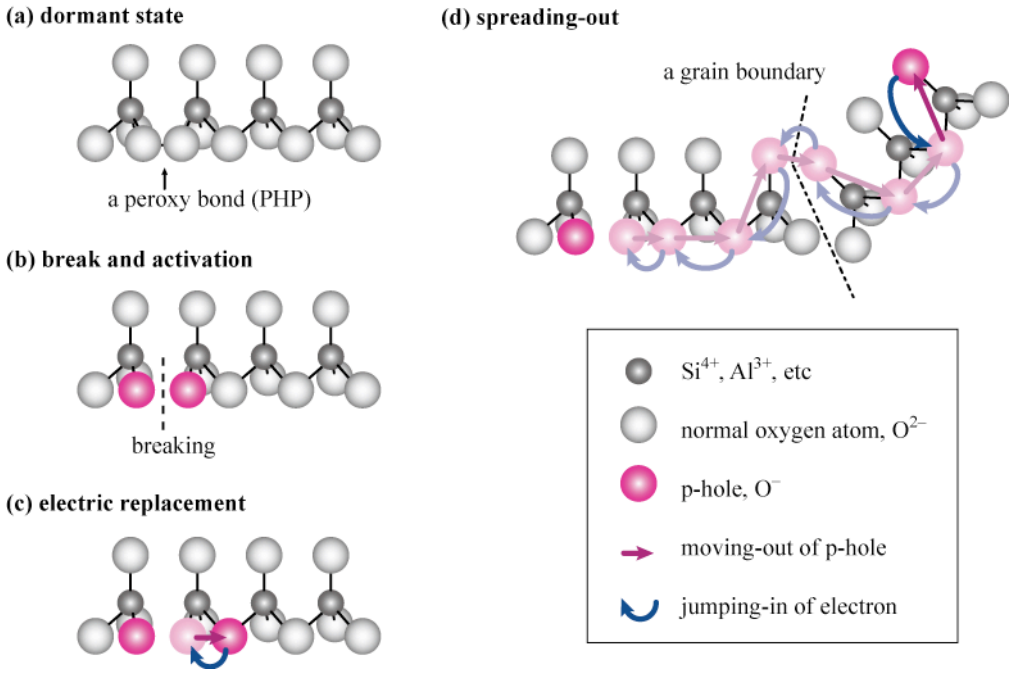

Fig. 1. Schematics of p-hole activation and spreading in igneous or high-grade metamorphic rock. (a) The p-holes equivalent to O^- are usually in a dormant state as spin-paired peroxy bonds that are also known as PHPs. (b) When stresses break a peroxy bond, two p-holes are activated. (c) An electron jumps in from a neighboring O^{2-} and the p-hole moves out. (d) The p-holes can spread across grain boundaries and through thick layers of igneous rocks.

type of electric charge carriers that may be suited to account for even very large telluric currents (e.g., Freund, 2000, 2002, 2003; Freund et al., 2004). In the following, we briefly review the source and nature of these charge carriers.

In the process of igneous rock formation that begins with the crystallization from H_2O-laden magmas, small amounts of water are structurally incorporated in the minerals, even into those that are normally considered anhydrous. The mode of incorporation includes the formation of hydroxyl, O_3X–OH with X = Si^{4+}, Al^{3+} etc. During cooling, hydroxyl pairs undergo an electronic rearrangement that leads to the formation of peroxy links, O_3X–OO–XO_3 (Fig. 1a). These links appear to be ubiquitous in all igneous and most high-grade metamorphic rocks. When such rocks are stressed, the peroxy links break (Fig. 1b), resulting momentarily in the formation of two non-bonding oxygens that have only 7 valence electrons instead of the usual 8. These oxygens can be viewed as O^-, but the more accurate representation is that of a missing electron, a "hole", in a matrix that consist of O^{2-}. When an electron from a neighboring O^{2-} jumps onto the O^- to fill the hole, this neighboring O^{2-} turns into an O^- (Fig. 1c). With this new O^-, a positively charged site has moved by one unit distance in the O^{2-} sublattice.

The p-hole moving process can repeat itself between O^- and more O^{2-} further out, allowing the O^- to move like a defect electron or hole in conventional p-type semiconductor. We call this O^- a positive hole (p-hole). Likewise we call the peroxy link a positive hole pair (PHP). The PHPs represent a dormant state of the p-holes. The p-holes can be activated by stress, which leads to dissociation of the PHPs. When this happens, the p-holes can spread out of the stressed volume because they can propagate through the valence band using the O 2p-dominated upper energy levels of the valence band by jumping from O^{2-} to O^{2-}. They can cross grain boundaries and thick layers of igneous rocks until they reach the surface (Fig. 1d). Thus, by placing igneous and high-grade metamorphic rocks under stress, we can produce currents of positive charge carriers that flow through these rocks although those rocks are usually good insulators. Details on p-holes and PHPs are given in Freund (2000, 2002, 2003) and Freund et al. (2004).

The spreading of p-holes through unstressed igneous rocks leads to two potentially important predictions: (i) when a portion of a rock is subjected to stress, the electrical conductivity in the unstressed portion of the rock should increase, and (ii) stressing produces self-generated currents that flow out of the stressed volume. In Section 2, to validate prediction (i), we pressed a central portion of rock tiles and measured the currents through the rock by applying a

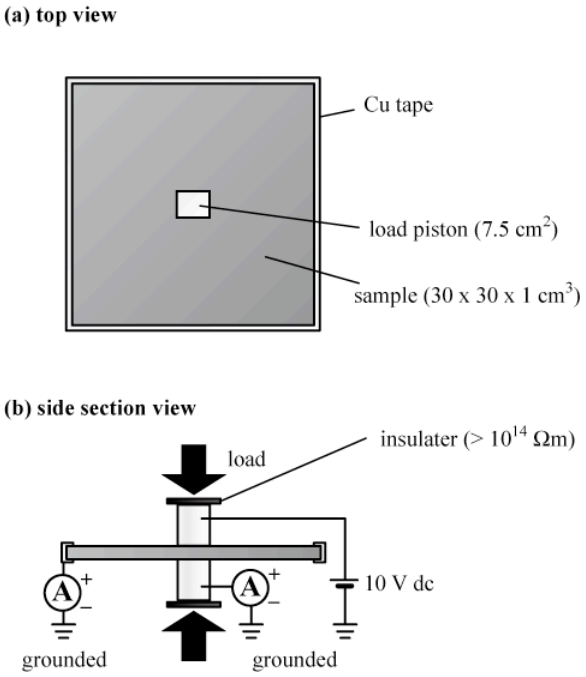

Fig. 2. Schematics of a set-up for uniaxial press tests to measure conductivity changes of stressed and unstressed volumes. (a) Top view. (b) Side cross section view.

dc voltage across the tiles. In Section 3, to validate prediction (ii), we used essentially the same experimental set-up but did not apply any external voltage. Instead we measured the self-generated currents and surface potentials. In Section 4, we discuss the consequences of our findings with respect to the behavior of p-holes in the Earth's crust and with respect to seismo-electromagnetic phenomena.

2. Conductivity change of stressed and unstressed volumes

An air-dry rock tile with a size of 30 x 30 x 1 cm^3 was used for the first set of experiments. The rock was a coarse-grained anorthosite that was a quartz-free igneous rock from Larvik, Norway. Figure 2 shows schematics of the experimental set-up that was placed inside a Faraday cage, using BNC cables for all external connections and additional shielding by wrapping Al foil around non-BNC wires. All four edges of the rock tile were covered with 12 mm wide Cu tapes with graphite-based conductive adhesive. They were acted as one electrode and connected to an ammeter (Model 486, Keithley). The center portion with a rectangular area of 2.5 x 3 cm^2 was uniaxially loaded with a pair of metal pistons that were insulated with high-density polyethylene sheets from the press (UTM-100, Industrial Process Controls Ltd.). A

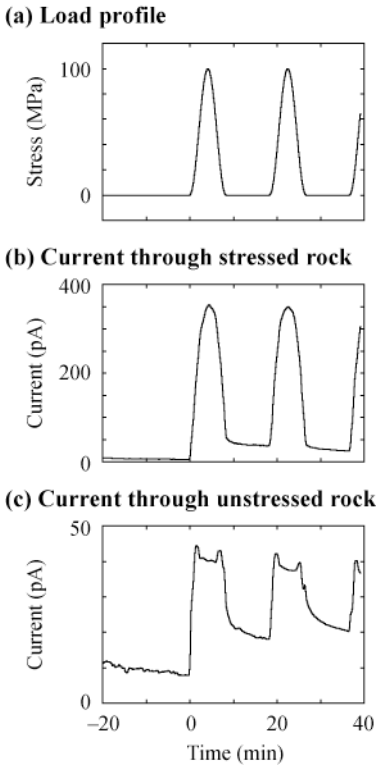

Fig. 3. A typical result. (a) Load profile. (b) Current from the top piston to the bottom piston through the central stressed volume. (c) Current from the central stressed volume through the surrounding unstressed volume to all edges.

+10 V dc voltage relative to ground was applied to the upper piston, while the lower piston was connected to a second ammeter (Model 617, Keithley). Two currents were measured during loading and unloading, one flowing from the biased piston to another piston through the central stressed volume and the other one from the biased piston to the edges of the rock tile. These two currents are indicators for the conductivity changes in the central stressed volume and the surrounding unstressed volume, respectively. For data acquisition, we used LabVIEW 7 installed on a custom-built PC running Windows 98.

Fig. 3a shows the load profile. The magnitude and period of the sinusoids were 0 to 100 MPa and 9 min, respectively. The sinusoidal loading was repeated at 10 min intervals. Application of the +10 V dc started 1 h before the start of loading. No audible or visible crack occurred during the tests. Figs. 3b and 3c show the currents through the stressed volume between the pistons and from the biased piston to the edge, respectively. Both currents increase upon first loading but do not come back upon unloading to their pre-loading baseline at repeated loading. When we remove the decreasing base line from the measured currents, each reloading produces the same currents

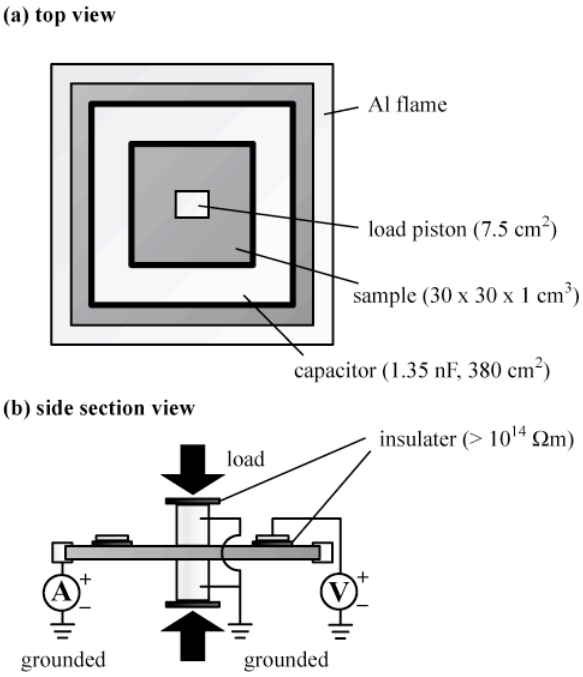

Fig. 4. Schematics of a set-up for uniaxial press tests to measure the self-generated currents and the surface potential. (a) Top view. (b) Side cross section view.

within experimental error. Although the loading followed a smooth sinusoidal curve, each current peak measured through the stressed volume exhibits slight depressions on its up and down slopes. Each current peak measured through the unstressed volume to the edges of the tile exhibits two bulges on both its up and down slopes. The sum of both currents gives a much smoother curve.

Because the geometry of the current paths and the rock volumes are different, we cannot normalize the piston-to-piston and piston-to-edge currents to compare and discuss them quantitatively. However, we can say that the increase of both currents indicates an increase in conductivity through both, the central stressed volume and the surrounding unstressed volume. Obviously, all other conditions being equal, the conductivity depends on the density of charge carriers. The results from the first series experiment therefore indicate that the density of charge carriers in the stressed and adjacent unstressed volumes increases with stress. The only place where the charge carriers can be reasonably assumed to be generated is the central stressed volume. Obviously, these charge carriers (or some of them) flow out into the surrounding unstressed volume. This leads to two questions: (1) Which types of charge curriers are generated and flow out? (2) Can the same charge carriers be expected to be generated and to flow in the Earth's crust? Since there are not externally applied bias voltages in the Earth's crust, we conducted the second series experiments to measure the self-generated currents.

3. Self-generation of positive currents

The same air-dry rock tiles with a size of 30 x 30 x 1 cm^3 were used for the second series of experiments. The rocks were a light-gray medium-grained granite and a black fine-grained gabbro. The granite is a quartz-rich igneous rock from Raymond, CA, and the gabbro is a quartz-free igneous rock from Shanxi, China. Fig. 4 shows schematically the set-up that was put into a Faraday cage. The rock tiles were fitted with 12 mm wide Cu tapes along all four edges and mounted in an aluminum frame. The frame was used as one electrode and connected to an ammeter (Model 486, Keithley). The central portion with a rectangular area of 2.5 x 3 cm^2 was uniaxially loaded with the same pistons as in the first series of experiments. Both pistons were insulated from the press with the same polyethylene sheets as mentioned above but were grounded. The current flowing from the central stressed volume through the surrounding unstressed volume to the edges of the tile was measured during loading and unloading. In addition, a capacitive sensor with an area of 380 cm^2 and a capacity of 1.35 nF was installed on the upper surface of the tiles surrounding the center portion. This capacitor was connected to a second electrometer (Model 617, Keithley) to measure the surface potential during loading and unloading.

Figs. 5a and 5d show the load profile common to the second series of experiments. The tiles were first loaded at 50 MPa for 3 h. Then, a sinusoidal loading of additional 10 MPa was superimposed and repeated at 2 min intervals. No audible or visible cracks occurred during the tests. Fig. 5 shows typical results from the granite and gabbro tiles. Both currents and the surface potential instantly increased to their maximums at the start of the initial loading. Both currents decreased slowly under constant load, while the surface potential decayed rapidly to its initial level. During the repetitive sinusoidal loading, both currents follow the applied stress, increasing and decreasing synchronously over the decaying base line.

The important point to note is that the currents are generated without any externally applied electric bias. The sign of the current flowing from the central stressed volume to the edges and the surface potentials are both positive. This means that positive charge carriers flow all by themselves from the central

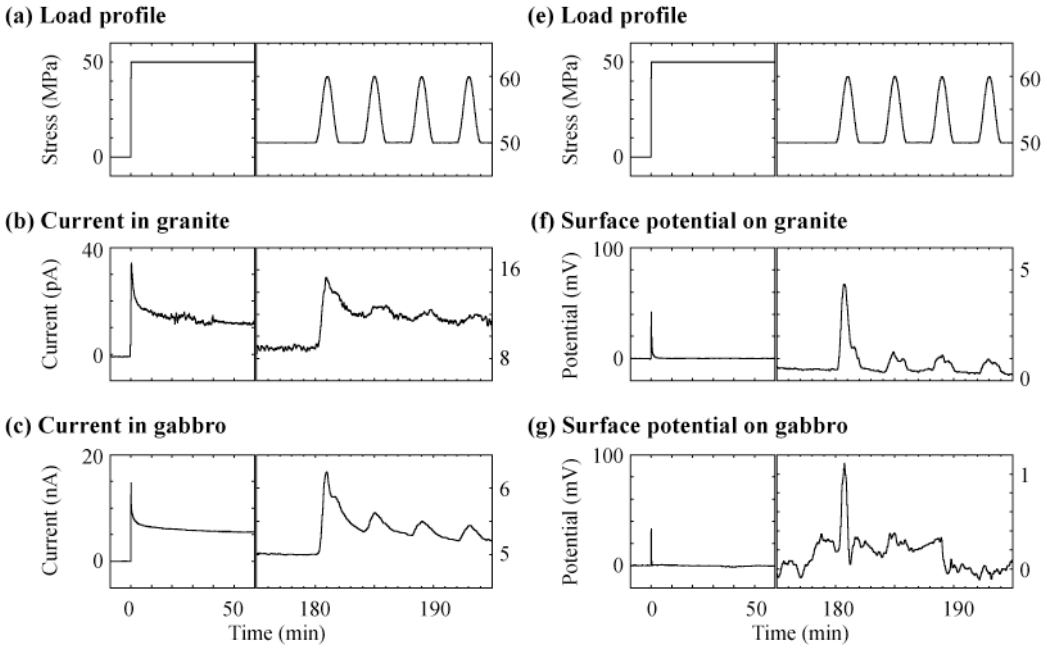

Fig. 5. Typical results. (a) Load profile. (b) Current in granite. (c) Current in gabbro. (d) Load profile, same with (a). (e) Surface potential on granite. (f) Surface potential on gabbro.

stressed volume to the edges traversing the surrounding unstressed volume. The magnitude of the current coming out of granite is significantly smaller than that coming out of gabbro, suggesting that the quartz grains in granite do not make a contribution through their piezoelectricity. In addition, since all rock samples were air-dry, there is no possibility that streaming potentials would be the source of the currents. However, if we consider p-holes as the active charge carriers (Fig. 1), we can explain all salient features of the experiment: the activation of p-holes in the central stressed volume, their outflow into the surrounding unstressed volume, and the appearance of a positive surface potential.

When we repeated the experiments with tiles of limestone, marble, and glass (30 x 30 x 1 cm^3), we observed lower, much lower, and no currents, respectively. This is consistent with the expectation that carbonate minerals such as calcite in limestone and marble do not contain PHPs and, hence, are unable to activate p-holes (Freund et al., 2004). In the case of glass, the concentration of peroxy links is probably below the detection limit.

4. Discussion and conclusion

Under the experimental set-up similar with that for the second series of experiments (Fig. 6), an extra ammeter placed between the metal pistons and the ground showed the mirror image of the current detected by the other ammeter between the edges and the ground (Fig. 7). This means that, in addition to the p-hole current flowing from the central stressed

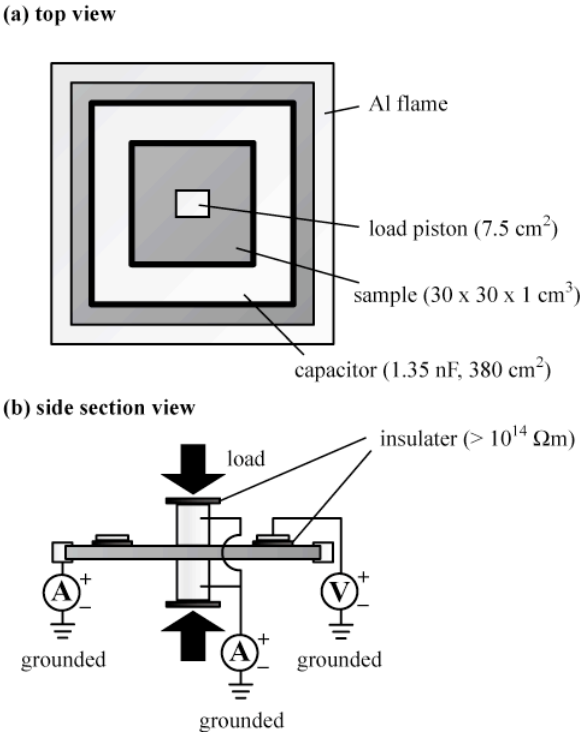

Fig. 6. Schematics of a set-up for uniaxial press tests to measure the two self-generated currents and the surface potential. (a) Top view. (b) Side cross section view.

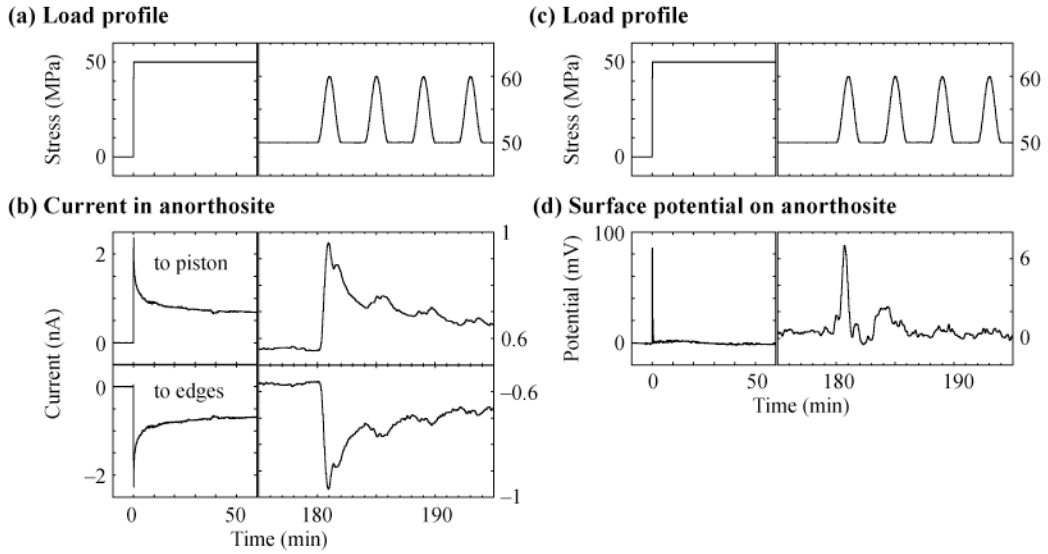

Fig. 7. Typical results. (a) Load profile, same with Figs. 5a and 5d. (b) Currents in anorthosite. (c) Load profile, same with (a). (d) Surface potential on anorthosite.

volume to the edges of the rock tile, the stressed volume releases an electron current of equal magnitude flowing out through the pistons. This also means that p-holes and electrons are activated at the same time. While the p-holes flow out through the unstressed volume, the electrons cannot stay behind because this would create a very large electric field. In order for the rock tile to remain electrically neutral, the electrons have to flow out as well. Since they can not flow through the unstressed volume, their only path is through the metal pistons in contact to the stressed volume. Thus, a stressed igneous rock behaves like a stress-current transformer. The boundary between the central stressed volume and the surrounding unstressed volume acts like a diode which permits p-holes to pass through the boundary but blocks electrons. Although the detailed mechanism is still unknown (e.g., what decides the flow directions of p-holes and electrons?), the stress or strain gradient may be one of the most important factors.

Teisseyre et al. (2001) conducted press tests using cylinders of tuff and limestone. Cylinders under uniaxially homogeneous loading generated transient increase and subsequent relaxation of currents (polarization). To explain the currents, they considered changes in the dislocation system: polarization due to charged edges on moving dislocations (Hadjicontis and Mavromatou, 1994, 1995) in addition to piezoelectric effect. On the other hand, Varotsos et al. (2001) conducted press tests using a cylinder of peridotite and a prismatic block of limestone. Both samples under inhomogeneous loading generated slowly decaying currents similar to our observations. To explain the currents, they considered the generation of free charges from electrically charged jogs on dislocations moving under the applied stress gradient (Fischbach and Nowick, 1955, 1958). The current magnitude detected was in agreement with signals detected in Greece before earthquakes, known as Seismic Electric Signals (SES). The relationship between moving dislocation and charge generation is concordant with p-hole activation in the central stressed volume. When dislocations move under stress and pass near PHPs, the PHPs can be cut and p-holes will be activated (Freund et al., 2004). P-hole's activation in a focal zone and subsequent flow into the surrounding rocks represents a possible source of SES as suggested earlier (e.g., Freund, 2000; Section 12.4.5 in Varotsos, 2005) although the magnitude of the current activated in limestone is lower than that in igneous rocks (Fig. 5).

In our experiments, the central stressed volume of the granite tiles with a size of 2.5 x 3 x 1 cm^3 and a volume of about 10 cm^3 generated a p-hole and an electron currents on the order of 10^{-6} A during the stress change from 50 MPa to 60 MPa (Fig. 5c). Anorthosite and gabbro produced 10–50 times higher currents than granite, while limestone and marble produced 1/10–1/100 times. Stress and strain changes at or around fault zones before an earthquake (e.g., Gladwin et al., 1994; Gwyther et al., 1996; Linde et al., 1996) would similarly produce electric currents. The p-holes may flow out into the surrounding ground. When we simply extrapolate our laboratory values to a stressed fault zone with a size of 10 x 10 x 10 km^3, such a rock volume will generate currents on the order of 10^4 A for granite (10^5 for anorthosite, 5 x 10^5 for gabbro, and 10^3 A for limestone). Under a

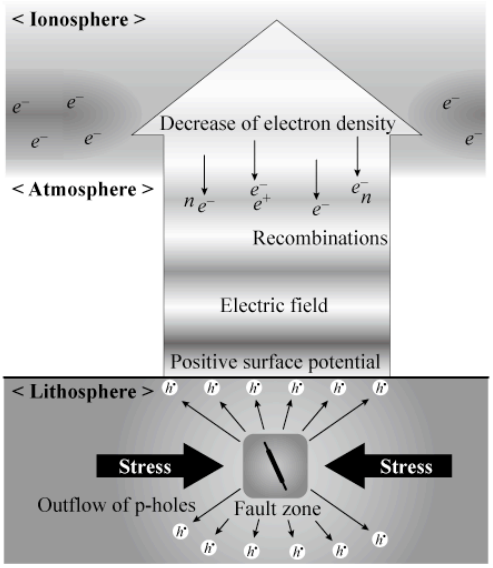

Fig. 8. The electrostatic channel for modeling of ionospheric perturbations. P-holes "$h^{\bullet}$" are activated in a stressed fault zone and spread out into the surrounding ground. Some of them reach the ground surface and form a positive ground surface potential over a large area around the epicenter. This potential causes a vertical electric field upward that penetrates the ionosphere through the atmosphere. The electrons "e^{-}" in the ionosphere are forced downward and recombine with neutral particles "n" or positive ions "e^{+}" in the atmosphere, affecting the electron (plasma) density in the ionosphere.

simplified assumption that this current flows out radially without loss, we might expect currents on the order of 10^{-4} A/m^2 at a distance of 100 km from the fault zone. Such current can influence conductivity measurements of the ground, cause abnormal magnetic fields, and emit low frequency electromagnetic emissions.

A portion of the p-holes will reach the ground surface and will build up a positive surface potential. In our experiments, the potential creates an electric field upward on the order of 10^2 V/m as estimated from our surface potential data and the area and capacity of the capacitive sensor. If a similar electric field builds up on the ground surface around an epicenter, it can be expected to lead to ionospheric perturbations upward the epicenter (Fig. 8) as suggested by Liu et al. (2001), Freund et al. (2004), and Kamogawa et al. (2004). For modeling ionospheric perturbations, three channels have been discussed (e.g., Hayakawa et al., 2004): the chemical channel (e.g., Sorokin et al., 2001; Rapaport et al., 2004), the acoustic channel (e.g., Shalimov and Gokhberg, 1998; Singh et al., 2004), and the electromagnetic channel (e.g., Molchanov et al., 1995; Grimalsky et al., 1999). Based on our results with p-holes as stress-activated charge carriers, we propose as a forth possibility "the electrostatic channel". In addition, we note that the electric fields created by the surface potential will be highest at sharp corners and edges where the radius of curvature is small. At these places, corona discharges are expected to occur at the ground-to-air interface as observed by Kamogawa et al. (2004) before earthquakes. On the other hand, p-holes recombining at the ground surface lead to vibrationally excited states and can release the excess energy as infrared (IR) emissions in the 10–11.5 μm range (Ouzonov and Freund, 2004). This mid-IR emission may account for the so-called thermal anomalies before earthquakes identified in satellite images (e.g., Tronin et al., 2002; Ouzonov and Freund, 2004).

There is a thermal gradient in the Earth's crust as well as a stress gradient. The temperature may reach 300–400 ºC at 10–20 km depth where typical focal zones are. On the other hand, p-holes can be thermally activated at 400–600 ºC (Freund 2003). Therefore, we can expect that p-holes may not yet be thermally activated in and around focal zones at these typical depths although we did not yet measure p-hole currents under the combined effect of temperature and confining pressure. The thermal gradient would be another important factor to decide the flow directions of p-holes. If stress or strain gradients and the thermal gradient affect the flow direction of p-holes activated in and around focal zones, the p-holes would tend to move upward and/or horizontally in the Earth's crust rather than downward. The crust, of course, is composed by various kinds of rocks (igneous and non-igneous) and includes water or brines in pores, fissures, and aquifers. In order to model p-hole currents in such complicated crustal environments, we need to know more about their behavior, tendency, and flow mechanisms under various conditions. So far we have still only limited information about PHPs and p-holes in laboratory-size samples.

Through laboratory experiments, we have recognized that the flow of p-holes in and out of stressed igneous rocks may represent an important and possibly widely applicable mechanism that operates in the Earth's crust when stresses build up. We therefore have to consider ground currents carried by p-holes as lithospheric source of seismo-electromagnetic phenomena in the lithosphere, atmosphere, and ionosphere. The p-hole currents can potentially be very powerful and would have to be taken into consideration in addition to or instead of competing concepts based on piezoelectricity, streaming potentials, gas emanations, and tribological electromagnetics.

Acknowledgements

We are supported by the NASA Ames Research Center Director’s Discretionary Fund (NASA Ames DDF), the National Imagery and Mapping Agency (NIMA), and the Japan Society for the Promotion of Science (JSPS) for Young Scientists. We thank C. Schwartz and N. Gibson at University of Maryland College Park for their technical support.

References

Enomoto, Y., Hashimoto, H., 1990. Emission of charged particles from indentation fracture of rocks. Nature 346, 641–643.

Fischbach, D.B., Nowick, A.S., 1955. Deformation-induced charge flow in NaCl crystals. Phys. Rev. 99, 1333–1334.

Fischbach, D.B., Nowick, A.S., 1958. Some transient electrical effects of plastic deformation in NaCl crystals. J. Phys. Chem. Solids 5, 302–315.

Freund, F., 2000. Time-resolved study of charge generation and propagation in igneous rocks. J. Geophys. Res. B 105, 11,001–11,019.

Freund, F., 2002. Charge generation and propagation in igneous rocks. J. Geodyn. 33, 543–570.

Freund, F., 2003. On the electrical conductivity structure of the stable continental crust. J. Geodyn. 35, 353–388.

Freund, F.T., Takeuchi, A., Lau, B.W.S., Post, R., Keefner, J., Mellon, J., Al-Manaseer, A., 2004. Stress-induced changes in the electrical conductivity of igneous rocks and the generation of ground currents. Terr. Atmosp. Ocean. Sci. 1, 437–467.

Gladwin, M.T., Gwyther, R.L., Hart, R.H., Breckenridge, K.S., 1994. Measurements of the strain field associated with episodic creep events on the San Andreas fault at San Juan Bautista, California. J. Geophys. Res. B 99, 4559–4565.

Gokhberg, M.B., Mogounov, V.A., Pokhotelov, A.O., 1995. Earthquake Prediction: Seismo-Electromagnetic Phenomena. Gordon and Breach Publishers, Singapore, 193 p.

Grimalsky, V.V., Kremenetsky, I., Chemnykh, O.K., Rapoport, Y., 1999. Excitation of electromagnetic waves in the lithosphere and their penetration into ionosphere and magetsphere, J. Atmos. Electr. 19, 101–117.

Gwyther, R.T., Gladwin, M.T., Mee, M., Hart, R.H.G., 1996. Anomalous shear strain at Parkfield during 1993-94. Geophys. Res. Lett. 23, 2425–2428.

Hadjicontis, V., Mavromatou, C., 1994. Transient electric signals prior to rock failure under uniaxial compression. Geophys. Res. Lett. 21, 1687–1690.

Hadjicontis, V., Mavromatou, C., 1995. Electric signals recorded during uniaxial compression of rock samples: their possible correlation with pre-seismic electric signals. Acta Geophys. Pol. 43, 49–61.

Hayakawa, M. (Ed), 1999. Atmospheric and Ionospheric Electromagnetic Phenomena Associated with Earthquakes. Terra Sci. Pub., Tokyo, 996 p.

Hayakawa, M., Molchanov, O.A. (Eds), 2002. Seismo Electromagnetics, Lithosphere-Atmosphere-Ionosphere Coupling. Terra Sci. Pub., Tokyo, 477 p.

Hayakawa, M., Molchanov, O.A., NASDA/UEC team, 2004. Summary report of NASDA’s earthquake remote sensing frontier project. Phys. Chem. Earth 29, 617–625.

Kamogawa, M., Liu, J.Y., Fujinawa, H., Chuo, Y.J., Tsai, Y.B., Hattori, K., Nagao, T., Uyeda, S., Ohtsuki, Y.H., 2004. Atmospheric field variations before the March 31, 2002 M6.8 earthquake in Taiwan. Terr. Atmosp. Ocean. Sci. 15, 397–412.

Kormiltsev, V.V., Ratuchnyak, A.N., Shapiro, V.A., 1998. Three-dimensional modeling of electric and magnetic fields induced by the fluid flow movement in porous media. Phys. Earth Planet. Inter., 105, 109–118.

Linde, A.T., Gladwin, M.T., Johnston, M.J.S., Gwyther, R.T., Bilham, R.G., 1996. A slow earthquake sequence on the San Andreas fault. Nature 383, 65–68.

Liu, J., Chen, Y.L., Chuo, Y.J., Tsai, H.F., 2001. Variation of ionospheric total electronic content during the Chi-Chi earthquake. Geophys. Res. Lett. 28, 1383–1386.

Mizutani, H., Ishido, T., Yokokura, T., Ohnishi, S., 1976. Electrokinetic phenomena associated with earthquakes, Geophys. Res. Lett. 3, 365–368.

Molchanov, O.A., Hayakawa, M., Rafalsky, V.A., 1995. Penetration characteristics of electromagnetic emission from an underground seismic source into the atmosphere, the ionosphere, and magnetosphere. J. Geophys. Res. A 100, 1691–1712.

Ogawa, T., Utada, H., 2000. Coseismic piezoelectric effects due to a dislocation 1. An analytic far and early-time field solution in a homogeneous whole space. Phys. Earth Planet. Inter. 121, 273–288.

Ouzonov, D., Freund, F., 2004. Mid-infrared emission prior to strong earthquakes analyzed by re-

mote sensing data. Adv. Space Res. 33, 268–273.

Pulinets S.A., Boyarchuk, K.A., Hegai, V.V., Kim, V.R., Lomonosov, A.M., 2000. Quasielectrostatic model of atmosphere-thermosphere-ionosphere coupling. Adv. Space Res. 26, 1209–1218.

Pulinets, A., Boyarchuk, K., 2004. Ionospheric Precursors of Earthquakes. Springer, Heidelberg, 289 p.

Rapoport, Y., Grimalsky, V., Hayakawa, M., Ivchenko, V., Juarez-R, D., Koshevaya, S., Gotynyan, O., 2004. Change of ionospheric plasma parameters under the influence of electric field which has lithospheric origin and due to radon emanation. Phys. Chem. Earth 29, 579–587.

Shalimov, S., Gokhberg, M., 1998. Lithosphere-ionosphere couplingmechanism and its application to the earthquake in Iran on June 20, 1990. A review of ionospheric measurements and basic assumptions. Phys. Earth Planet. Inter. 105, 211–218.

Singh, B.V., Kushwah, V., Singh, O.P., Lakshmi, D.R., Reddy, B.M., 2004. Ionospheric perturbations caused by some major earthquakes in India. Phys. Chem. Earth 29, 537–550.

Sorokin, V.M., Chmyrev, V.M. Yaschenko, A.K., 2001. Electrodynamic model of the lower atmosphere and the ionosphere coupling. J. Atmosp. Solar-Terr. Phys. 63, 1681–1691.

Takeuchi, A., Nagahama, H., Hashimoto, T., 2004. Surface electrification of rocks and charge trapping centers. Phys. Chem. Earth 29, 359–366.

Teisseyre, R., 2001. Dislocation dynamics and related electromagnetic excitation. Acta Geophys. Pol. 49, 55–73.

Teisseyre, K.P., Hadjicontis, V., Mavromatou, C., 2001. Anomalous piezoelectric effect: analysis of experimental data and numerical simulation. Acta Geophys. Pol. 49, 449–462.

Tronin, A.A., Hayakawa, M., Molchanov, O.A., 2002. Thermal IR satellite data application for earthquake research in Japan and China. J. Geodyn. 33, 519–534.

Varotsos, P., 2005. The physics of Seismo Electric Signals. Terra Sci. Pub., Tokyo, 338 p.

Varotsos, P., Hdjicontis, V., Nowick, A., 2001. The physical mechanism of seismic electric signals. Acta Geophys. Pol. 49, 416–421.

Vershinin, E.F., Buzevich, A.V., Yumoto, K., Saita, K., Tanaka, Y., 1999. Correlation of seismic activity with electromagnetic emissions and variations in Kamchatka region. In: Hayakawa, M. (Ed). Atmospheric and Ionospheric Electromagnetic Phenomena Associated with Earthquakes. pp. 513–517, Terra Sci. Pub., Tokyo.

Yoshida, S., Ogawa, T., 2004. Electromagnetic emissions from dry and wet granite associated with acoustic emissions. J. Geophys. Res. 109, B09204.

(Submitted, June 2, 2005; Revised, October 3, 2005; Accepted, October 18, 2005)